Biochemical and Biophysical Research Communications 426 (2012) 409–414

Contents lists available at SciVerse ScienceDirect

Biochemical and Biophysical Research Communications

journal homepage: www.elsevier.com/locate/ybbrc

Development of a quantitative diagnostic method of estrogen receptor expression levels by immunohistochemistry using organic fluorescent material-assembled nanoparticles

Kohsuke Gonda [a,*], Minoru Miyashita [b], Mika Watanabe [c], Yayoi Takahashi [c], Hideki Goda [d], Hisatake Okada [d], Yasushi Nakano [d], Hiroshi Tada [b], Masakazu Amari [a], Noriaki Ohuchi [a,b]

[a] Department of Nano-Medical Science, Graduate School of Medicine, Tohoku University, Seiryo-machi, Aoba-ku, Sendai 980-8575, Japan
[b] Department of Surgical Oncology, Graduate School of Medicine, Tohoku University, Seiryo-machi, Aoba-ku, Sendai 980-8574, Japan
[c] Department of Pathology, Tohoku University Hospital, Seiryo-machi, Aoba-ku, Sendai 980-8574, Japan
[d] Optical and Biological R&D Center, Konica Minolta Technology Center, Inc., No. 1 Sakuramachi, Hino-shi, Tokyo 191-8511, Japan

ARTICLE INFO

Article history:
Received 19 August 2012
Available online 29 August 2012

Keywords:
Immunohistochemistry
Cancer
Estrogen receptor
Nanoparticle
Diagnosis
Quantitative sensitivity

ABSTRACT

The detection of estrogen receptors (ERs) by immunohistochemistry (IHC) using 3,3′-diaminobenzidine (DAB) is slightly weak as a prognostic marker, but it is essential to the application of endocrine therapy, such as aromatase inhibitor- or antiestrogen tamoxifen-based therapy. IHC using DAB is a poor quantitative method because horseradish peroxidase (HRP) activity depends on reaction time, temperature and substrate concentration. However, IHC using fluorescent material provides an effective method to quantitatively use IHC because the signal intensity is proportional to the intensity of the photon excitation energy. However, the high level of autofluorescence has impeded the development of quantitative IHC using fluorescence. We developed organic fluorescent material (tetramethylrhodamine)-assembled nanoparticles for IHC. Tissue autofluorescence is comparable to the fluorescence intensity of quantum dots, which are the most representative fluorescent nanoparticles. The fluorescent intensity of our novel nanoparticles was 10.2-fold greater than quantum dots, and they did not bind non-specifically to breast cancer tissues due to the polyethylene glycol chain that coated their surfaces. Therefore, the fluorescent intensity of our nanoparticles significantly exceeded autofluorescence, which produced a significantly higher signal-to-noise ratio on IHC-imaged cancer tissues than previous methods. Moreover, immunostaining data from our nanoparticle fluorescent IHC and IHC with DAB were compared in the same region of adjacent tissues sections to quantitatively examine the two methods. The results demonstrated that our nanoparticle staining analyzed a wide range of ER expression levels with higher accuracy and quantitative sensitivity than DAB staining. This enhancement in the diagnostic accuracy and sensitivity for ERs using our immunostaining method will improve the prediction of responses to therapies that target ERs and progesterone receptors that are induced by a downstream ER signal.

1. Introduction

The estrogen receptor (ER), progesterone receptor (PgR) and human epidermal growth factor 2 (HER2) were the first biomarkers for breast cancer to be recommended for routine clinical use. ER, PgR, and HER2 exhibit mixed prognostic and predictive values, depending on the treatment that is administered. ER is a member of the nuclear hormone family of intracellular receptors, and it plays a critical role in cancer growth. Approximately 70% of breast cancer cases are ER-positive [1–4]. Estrogen activates the ER, which binds to DNA and regulates the activity of many different cellular proliferation genes [1–5].

Pathological examination is the gold standard for cancer diagnosis, and it also contributes to the elucidation of cancer etiology, pathogenesis, clinicopathological correlations, and prognosis. The detection of ERs by immunohistochemistry (IHC) using 3,3′-diaminobenzidine (DAB) is slightly weak as a prognostic marker, but it is essential for the application of endocrine therapy, such as aromatase inhibitor- or antiestrogen tamoxifen-based therapy [1–4]. DAB-stained positive ER cell rates greater than 1%, 5%, and 10% are regarded as positive in some IHC methods in which the cells are not individually counted [2]. The Study Group of the Japanese Breast Cancer Society recommends a positive finding when 10% or more cells are ER-positive and a lower rate as borderline [2], but the staining intensity of DAB is not considered. The Allred

* Corresponding author.
E-mail address: gonda@med.tohoku.ac.jp (K. Gonda).

0006-291X/$ - see front matter © 2012 Elsevier Inc. All rights reserved.
http://dx.doi.org/10.1016/j.bbrc.2012.08.105

score, which is another judging method, assesses DAB staining intensity in the nuclei of cancer cells [2]. However, the staining intensity is categorized into only four degrees (none, weak, intermediate, and strong) using visual judgment. Therefore, the quantitative sensitivity of diagnosis is low, resulting in differing views of diagnosis.

IHC with DAB (IHC-DAB) is the most conventional IHC protocol. However, the intensity of DAB staining depends on the enzyme activity of horseradish peroxidase (HRP). Therefore, the staining intensity is significantly influenced by reaction time, temperature and HRP substrate concentrations. The intensity of DAB staining often differs between experimenters. IHC using fluorescent molecules or particles as labels is an effective quantitative use of IHC because the intensity of fluorescent materials is proportional to the intensity of photon excitation energy, which is an irreversible chemical reaction. However, high levels of tissue autofluorescence have impeded the development of this technique. Quantum dots (QDs) [6] are fluorescent nanoparticles that exhibit greater photostability and brightness than general organic fluorescent molecules, such as FITC, rhodamine, and Alexa Fluors. QD fluorescence is sufficient for cultured cell imaging because the autofluorescent intensity of cultured cells is low [6]. However, tissue autofluorescence is comparable to the fluorescent intensity of QDs. Therefore, a quantitative analysis using only the fluorescent intensity of QDs while excluding tissue autofluorescence is difficult.

The creation of a novel bright fluorescent material suitable for IHC was required to improve fluorescent labeling IHC for the quantitative diagnosis of ER expression. We prepared organic fluorescent material-assembled nanoparticles for IHC. The fluorescent intensity of the novel nanoparticles was approximately 10-fold greater than that of QDs, and the level of ER expression was quantified with much greater accuracy compared to IHC-DAB. This method will improve the diagnosis of ER for endocrine therapy.

2. Materials and methods

2.1. Preparation of organic fluorescent material-assembled nanoparticles for IHC

The methods of previous studies [7,8] were extensively improved in this study to prepare the organic fluorescent material-assembled nanoparticle, and the following new method was developed. Tetramethylrhodamine (TMR, 6.6 mg) (GE Healthcare) was mixed with 3 μl 3-aminopropyltriethoxysilane (ShinEtsu) in dimethylformamide. This mixture (0.6 ml) was incubated with a buffer containing 48 ml of ethanol, 0.6 ml of tetraethylorthosilicate, 2 ml of ultrapure deionized water, and 2 ml of ammonia water for 3 h. The incubated sample was centrifuged at 10,000×*g* for 20 min. The precipitates were washed with ethanol and water using centrifugation. TMR-assembled nanoparticles were obtained using this process. To coat the surface of TMR-assembled nanoparticles with streptavidins via polyethylene glycol (PEG) chains, 3 nM TMR-assembled nanoparticles were treated with one of the PEG chains, succinimidyl-[(-maleomidopropionamid)-dodecaethyleneglycol] ester (Thermo Fisher Scientific, Inc.), in phosphate-buffered saline (PBS) containing EDTA for 1 h. The PEG chain-coated TMR-assembled nanoparticles were centrifuged at 10,000×*g* for 20 min. The precipitates were washed with PBS containing EDTA using centrifugation. The sample was incubated with streptavidins reduced by dithiothreitol for 1 h. The sample was washed and redispersed in PBS containing 2 mM EDTA. Streptavidin-coated TMR-assembled nanoparticles (Avi-TMR particles) were obtained for immunostaining.

2.2. Evaluation of Avi-TMR particle characteristics

The Avi-TMR particle was measured using a scanning electron microscope (SEM) (S-4800, Hitachi). The Avi-TMR particle suspension for SEM was directly applied to the collodion-coated copper grid. We measured the diameter of more than 1000 particles. The diameter of the Avi-TMR particle was also analyzed using Dynamic Light Scattering (DLS) (Zetasizer Nano, Malvern Instruments, Ltd.). The emission fluorescence spectrum of the nanoparticles was measured with a spectrometer (F-7000, Hitachi) to investigate the fluorescent properties of the Avi-TMR particles.

2.3. Immunostaining

Breast cancer tissue specimens that expressed estrogen receptors (ER) at high or low levels were purchased from a medical supply manufacturer (US Biomax, Inc.). The specimens were deparaffinized in xylene and hydrated in graded alcohols and distilled water. Endogenous horseradish peroxidase (HRP) activity was blocked by incubation in methanol containing 0.3% hydrogen peroxide for 20 min at 25 °C. The specimens were washed with distilled water, and antigen retrieval was performed using an autoclave in 10 mM citrate buffer (pH, 6.0) and heat (121 °C) for 5 min. The samples were incubated with 1% BSA for 1 h at 25 °C and immunostained using 6 mg/ml of a rabbit anti-ER primary antibody (Roche) for 1 h at 25 °C. The samples were washed with PBS and incubated with a biotinylated goat anti-rabbit IgG secondary antibody. The samples were incubated with streptavidin-conjugated HRP (Vector Labs.) for 30 min at 25 °C or Avi-TMR particles for 2 h at 25 °C. Samples that were incubated with streptavidin-conjugated HRP were treated with a DAB chromogen reagent (Roche). DAB chromogen treatment was concurrently performed under the same conditions (temperature, time, and substrate concentration) in all tissues. The reaction of all tissues, including low-level ER-expressing samples, was arrested according to the manufacturer's instructions when a strong DAB intensity was recognized in tissues with high-level ER expression. In addition to the staining of biomarkers, the investigation of nuclear morphology using counterstaining with hematoxylin is very important in cancer diagnosis using IHC. All samples were stained with hematoxylin after DAB and Avi-TMR particle staining and mounted in a mounting medium for observation.

2.4. Optical systems

Two types of optical systems were used in this study. One optical system observed the fluorescence of QDs and consisted primarily of an epi-fluorescent microscope (IX-71, Olympus) with modifications, a Nipkow disk-type confocal unit (CSU10, Yokogawa), and an electron multiplier type charge-coupled device camera (EM-CCD, Ixon DV887, Andor Technology), which is highly sensitive camera [9,10]. A PlanApo (X60, 1.40 NA, Olympus) objective lens was used for imaging. This system compared the fluorescent intensity of Avi-TMR particles to QDs. The other optical system was a light microscopy (BX51, Olympus, Japan) equipped with a camera (DP2-BSW, Olympus). This general-purpose microscope visualized Avi-TMR particles and color images in DAB staining, but it did not visualize QDs due to the low sensitivity of camera. This system was used for the data analysis of IHC using DAB or Avi-TMR particles.

2.5. Data analysis of immunostaining with DAB or Avi-TMR particles

The following data analyses were performed to quantitatively measure the intensity of DAB and Avi-TMR particle staining. DAB stained images were converted into a gray scale JPEG image, and

the gray scale tone was inverted to produce a high DAB staining intensity, which was visualized as a high gray value in the 256 gray level. Black and white was defined as values of 0 and value 255, respectively, in the 256 gray level scale (8 bits per pixel). The nuclear region was surrounded by a region of interest (ROI) to measure the DAB staining intensity in each cell nucleus, and the mean gray value per pixel in the ROI was calculated using Image J software (http://www.rsb.info.nih.gov/ij/).

Avi-TMR particle stained images were converted into gray scale JPEG images to produce high fluorescent intensities that were visualized as high gray values in the 256 gray level. Gray level correction was applied to the images using the level correction function in Photoshop (Adobe) to exclude the effect of autofluorescence from the analysis of Avi-TMR particle-derived fluorescence signals. The nuclear region was surrounded with an ROI that was determined by the hematoxylin staining of the nucleus in the identical specimen to measure the Avi-TMR particle-derived fluorescent intensity in each cell nucleus. The mean gray value per pixel in the ROI was calculated using Image J software.

The value of each datum was multiplied by a constant coefficient to compare DAB and Avi-TMR particle staining intensity on the same scale, and the mean value of each data set was adjusted to 100 in arbitrary units (a.u.). More than 100 cells from the same region of adjacent tissues were examined in these data comparisons.

3. Results and discussion

3.1. Avi-TMR particle preparation and characteristics evaluation

IHC-DAB is a poor quantitative method because HRP activity depends on reaction time, temperature and substrate concentrations. Therefore, the intensity of DAB staining often varies between experimenters. IHC using fluorescent molecules or particles is an effective quantitative use of IHC because the fluorescent intensity of the materials is proportional to the intensity of photon excitation energy. However, tissue samples exhibit autofluorescence of various intensities. The high levels of autofluorescence have impeded the development of quantitative fluorescent IHC because these high intensities produce false positive signals. The fluorescent intensity of general organic fluorescent molecules, such as FITC, rhodamine, and Alexa Fluor, cannot exceed the autofluorescence of tissues. QDs [6] are brighter fluorescent materials than general organic fluorescent molecules. However, the fluorescence intensity of QDs does not exceed the autofluorescence intensity of all tissues. Therefore, the creation of a novel bright fluorescent material suitable to IHC was required.

We selected an organic fluorescent molecule, tetramethylrhodamine (TMR), and we prepared streptavidin-coated "TMR-assembled nanoparticles" (Avi-TMR particles). The Avi-TMR particle consisted of hundreds of thousands of TMRs, and its surface was coated with streptavidins via PEG chains (Fig. 1A). The diameters of more than 1000 Avi-TMR particles were measured using SEM. The SEM image (Fig. 1B) revealed that the TMR particles were quite uniform in size, and the average size was 115 nm (variation coefficient, 12%) (Fig. 1C). The diameter size of Avi-TMR particles was also examined using DLS. The peak value in the particle size distribution data was 112 nm, which demonstrated that the DLS data were similar to the SEM data (Fig. 1D).

The emission fluorescence spectra of the nanoparticles were measured with a spectrometer to investigate the fluorescence properties of Avi-TMR particles. The fluorescence spectral analysis demonstrated that the 532 nm light-excited spectral patterns of the TMR and Avi-TMR particles were nearly identical, and the fluorescence intensity for both particles peaked at approximately 580 nm (Fig. 1E). These data indicated that our nanoparticle prep-

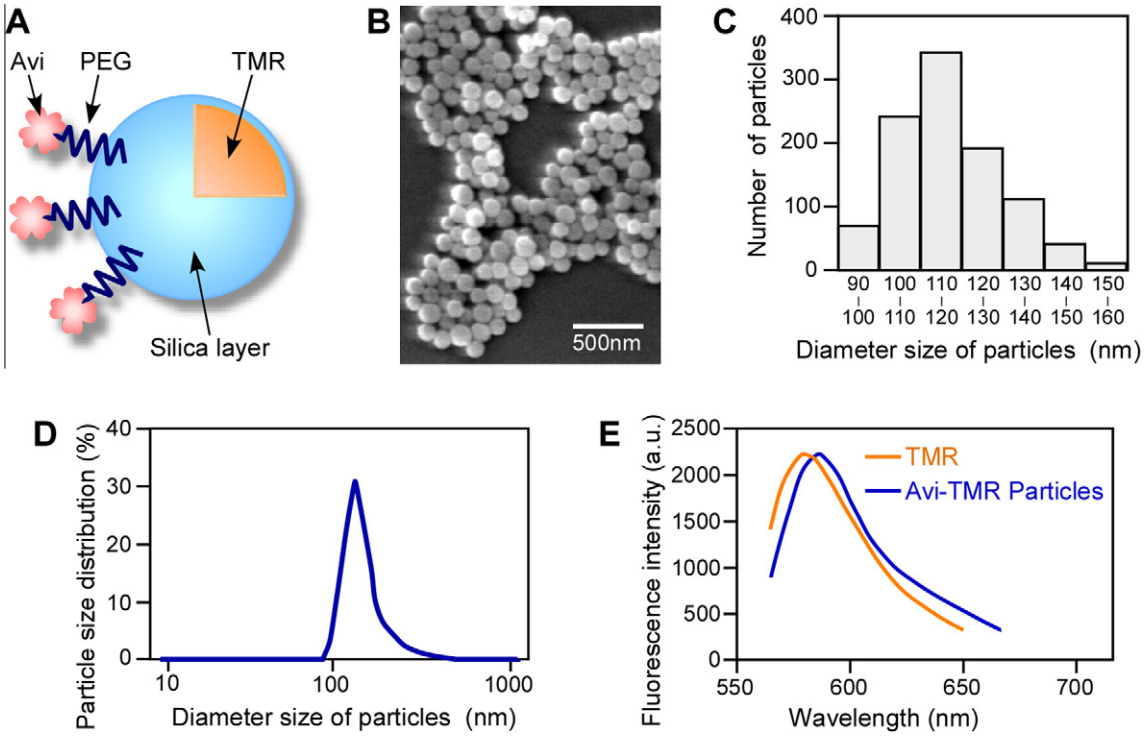

Fig. 1. Avi-TMR particle preparation and characteristics evaluation. (A) Schematic for the Avi-TMR particle preparation. Avi, streptavidin; PEG, polyethylene glycol chain; TMR, tetramethylrhodamine; Silica layer was made from tetraethylorthosilicate. (B) SEM image of Avi-TMR particles. (C) Distribution of diameter sizes of Avi-TMR particles in SEM image. Average size was 115 nm, and variation coefficient was 12%. (D) DLS data for Avi-TMR particles. In the particle size distribution data, the peak value was 112 nm. (E) The 532 nm light-excited fluorescence spectra of TMR only and Avi-TMR particles.

aration method did not affect the spectral patterns of the TMR. The fluorescent intensity of Avi-TMR particles was compared to that of Qdot 655 (Life Technologies Co.) using a spectrometer (the model number indicates the emission wavelength). Qdot 655 is the brightest QD from this company following excitation with a 532 nm laser. QDs are excited by various wavelengths below the emission wavelength, and they are more effectively excited by a short wavelength than a long wavelength. Therefore, the peak values of fluorescent intensity between 365 nm light-excited Qdot655 and 532 nm light-excited Avi-TMR particles were compared using a spectrometer. The results demonstrated that the peak fluorescent intensity value of Avi-TMR particles was 10.2-fold greater than that of 365 nm-excited Qdot655. Additionally, an optical system for the fluorescent observation of QDs yielded similar results. These data suggested that the Avi-TMR particles possessed a significantly higher fluorescence intensity than the autofluorescence intensity of tissues.

3.2. Immunostaining of ER with Avi-TMR particles in breast cancer tissues

The detection of ER using IHC in breast cancer tissue is a slightly weak prognostic marker of clinical outcomes, but it is a strong predictive marker for the response to hormone-based therapies, such as aromatase inhibitor or tamoxifen [1–4]. The Study Group of the Japanese Breast Cancer Society recommends a positive judgment when more than 10% of DAB-stained ER-positive cells are present in tissues [2]. However, the DAB staining intensity of each cell is not considered. The Allred score, which is another assessment method, considers DAB staining intensity, but the intensity is categorized into the only four degrees using visual judgment [2]. IHC-DAB is a poor quantitative method. Therefore, the quantitative sensitivity of the existing diagnostic methods for ER detection is quite low.

We purchased breast cancer tissue specimens that expressed ERs at high or low levels from a medical supply manufacturer and immunostained these tissues with Avi-TMR particles. Adjacent specimens were incubated with a rabbit anti-ER primary antibody after antigen retrieval and a goat anti-rabbit IgG secondary antibody. The samples were incubated with streptavidin-conjugated HRP or Avi-TMR particles. We observed differences in the quantitative sensitivity of DAB staining and fluorescent nanoparticle staining. ER is a member of the nuclear hormone family of intracellular receptors. Therefore, nuclear staining is observed in cancer cells that are positively immunostained with an anti-ER primary antibody. Fig. 2 illustrates the immunostaining patterns of DAB and Avi-TMR particles in high- and low-level ER-expressing tissues. DAB or Avi-TMR particle staining exhibited non-staining or weak staining intensity in low-level ER-expressing tissues, respectively (Fig. 2A and E) and strong intensity in high-level ER-expressing tissues (Fig. 2B and F). These results suggested that both IHC methods specifically stained ER-expressing breast cancer tissues. Tissue autofluorescence is comparable to the fluorescent intensity of QDs. However, the fluorescence intensity of Avi-TMR particles was 10.2-fold greater than that of Qdot655. Therefore, we obtained significantly higher signal-to-noise ratios for the Avi-TMR particles in the imaging data. In addition to the staining of biomarkers in cancer diagnosis using IHC, the investigation of nuclear morphology by counterstaining with hematoxylin is very important. Hematoxylin staining did not effect Avi-TMR particle staining patterns (Fig. 2C–F), which demonstrated that a biomarker diagnosis using Avi-TMR particles and nuclear morphology diagnosis using hematoxylin can be performed in identical tissue specimens (Fig. 2G and H).

3.3. Analysis of ER-immunostaining data with the Avi-TMR particle

DAB chromogen reagent reactions were arrested simultaneously in all tissues based on the reaction time of high-level ER-expressing tissues (see Section 2). However, DAB staining in low-level ER-expressing tissues was difficult to identify (Fig. 2A). Longer reaction times are required to clearly observe low expression levels of ER using DAB staining. Many pathology departments stain each tissue specimen with DAB, using different reaction times at seasonally influenced room temperatures. These situations prevent a quantitative analysis of DAB staining data. However, positive signals from Avi-TMR particles in low-level ER-expressing tissues were clearly observed, although the numbers of bright spots were present in small amounts (Fig. 2E and G). Non-specific

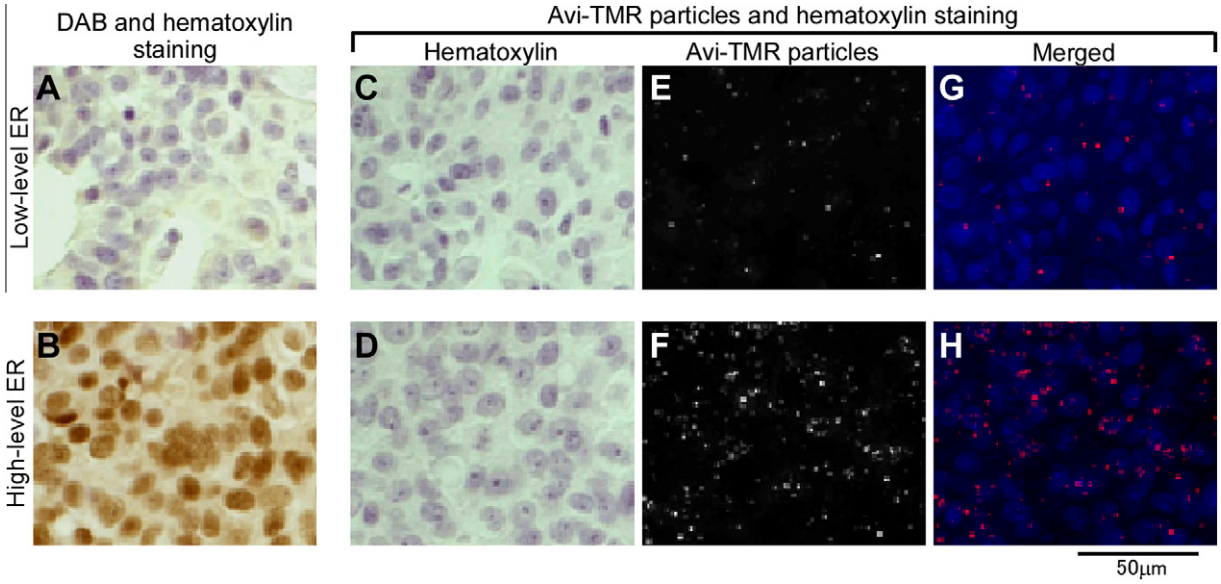

Fig. 2. Immunostaining of ER in breast cancer tissues with DAB or Avi-TMR particles. Breast cancer tissues that expressed ER at low (A, C, E, G) or high levels (B, D, F, H) were immunostained. The tissues shown in (A) and (B) were immunostained with DAB and counterstained with hematoxylin. The tissues shown in (C–H) were immunostained with Avi-TMR particles and counterstained with hematoxylin. (C) and (E) or (D) and (F) are double-stained images in same microscopic field of identical tissues, respectively. Images merged with (C) and (E) or (D) and (F) are shown in (G) or (H), respectively.

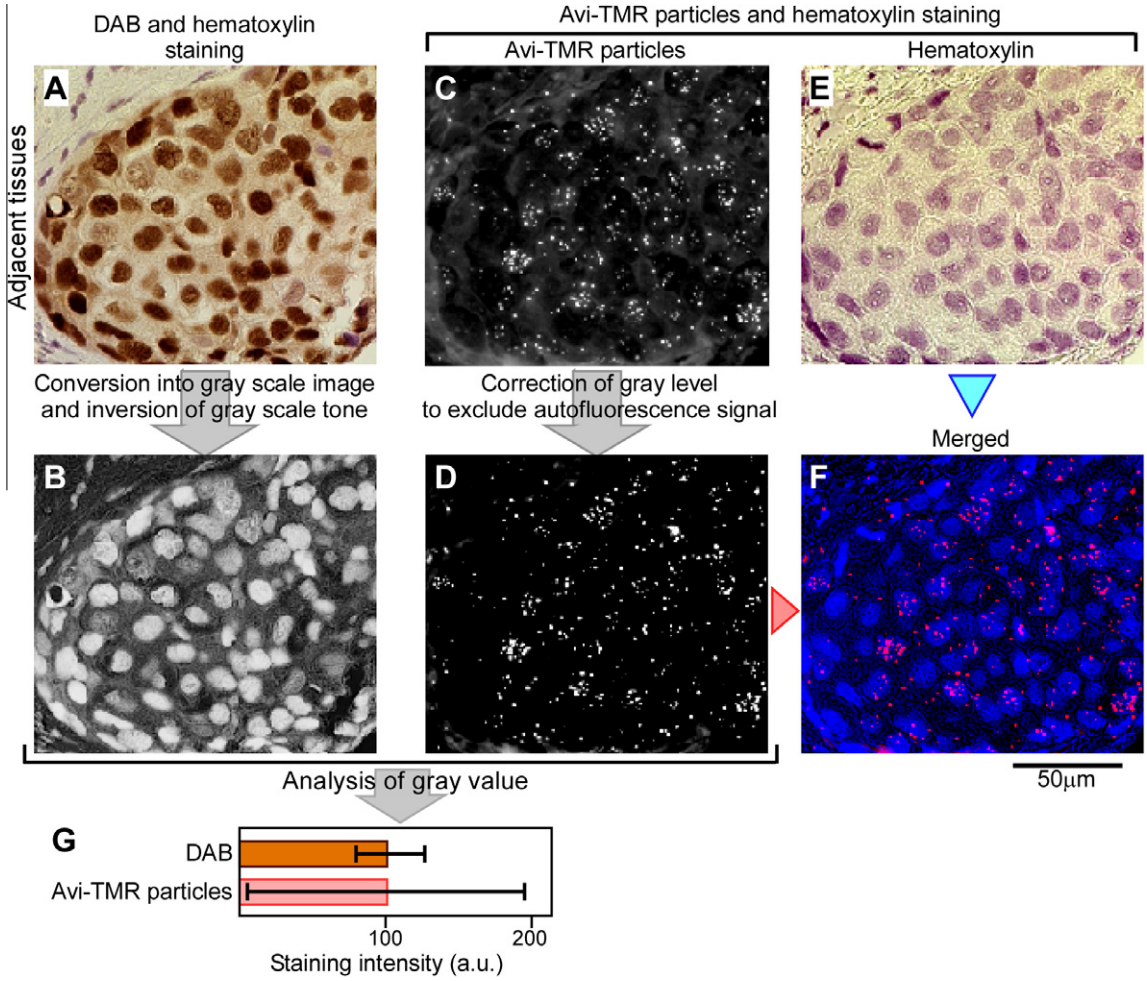

Fig. 3. Quantitative analysis of ER-immunostaining data with DAB or Avi-TMR particles. Adjacent tissues expressing ER at high levels were immunostained with DAB and hematoxylin (A) or Avi-TMR particles (C) and hematoxylin (E). The same regions in both tissues were observed. DAB staining image (A) was converted into a gray scale image, and the gray scale tone was inverted (B). As result of this, high DAB-staining intensity was visualized as a high gray value in the 256 gray level (B). Avi-TMR particle staining images were converted into gray scale images, and the gray level correction of the image was performed (D) to exclude the effect of autofluorescence. To measure the Avi-TMR particles fluorescent signal in cell nuclei, the nuclear region was surrounded with an ROI that was determined using the hematoxylin staining image (E). An image merged with (D) and (E) is shown in (F). The mean values of DAB staining intensity (B) or Avi-TMR particle staining intensity (D) were adjusted to 100 as an arbitrary unit (G). Error bars (G) indicate standard deviations that showed the wide range of variations in staining intensity values.

binding of Avi-TMR particles to the tissues was seldom observed due to the surface coating with PEG chains (data not shown). These results demonstrated that Avi-TMR particle staining quantitatively analyzed a wider range of ER expression levels compared to DAB staining.

Adjacent tissues that expressed high ER levels were immunostained with DAB or Avi-TMR particles to compare the quantitative sensitivity of the two methods, and the same regions of both tissues were observed (Fig. 3A and C). Cancer tissue cells exhibit different cell types and receive various heterogeneous signals in a complicated tissue structure that includes blood and lymph vessels and three-dimensional cellular communication systems [11,12]. Therefore, cancer tissue consists of a heterogeneous cell population, and each cell expresses proteins at different levels [11,12]. Previous studies did not consider the ER-expression levels of each cell. Therefore, it is difficult to diagnose ER levels with high accuracy and apply the pathological information to ER-targeted medical therapy. Fig. 3 illustrates that DAB and Avi-TMR particles stained the same regions in adjacent tissues. Each image (Fig. 3A and C) was converted into a gray scale image (Fig. 3B and D), and the staining intensity per cell nucleus was measured. A wide range of variations in nuclear size was observed in tissue sections (Fig. 3A, E and F). Therefore, the staining intensities were calculated as gray values per pixel in the cell nucleus to avoid a staining intensity value that depended on cell nuclear size. Moreover, the value of each data set was multiplied by a constant coefficient, and the mean value of each data set was adjusted to 100 as an arbitrary unit (a.u.) so that the DAB and Avi-TMR particle staining intensity data could be compared on the same scale (Fig. 3G). More than 100 cells in the same region in adjacent tissues were examined in these data comparisons. ER expression levels vary widely according to cell heterogeneity in tissues. Therefore, a wide range in staining intensity values may be produced by the accuracy and quantitative sensitivity of IHC. The results demonstrated that the standard deviations of Avi-TMR particle staining images was much larger than the DAB staining images (Fig. 3G). Avi-TMR particles do not bind non-specifically to cancer tissues. Therefore, bright spots of Avi-TMR particles in Fig. 3D are positive signals. These results demonstrate that the Avi-TMR particle-staining method greatly increased the accuracy and quantitative sensitivity of IHC compared to IHC-DAB. Enhancement of the diagnostic accuracy and quantitative sensitivity for ER will improve the predictive response to therapies targeting ERs and PgRs that are induced by a downstream ER signal. IHC techniques that incorporate the use of Avi-TMR parti-

cles may aid in the diagnostic efficacy for other molecular target therapies. Therefore, this new immunostaining method can be expected to contribute to the diagnosis of various cancers.

Acknowledgments

Part of this work was supported by a Grant-in-Aid for challenging Exploratory Research (21659144) by the Japan Society for the Promotion of Science (JSPS) (K. Gonda), Grant-in-Aid for Scientific Research (B) (24300336) by JSPS (K. Gonda), a Grant-in-Aid for Scientific Research in Innovative Areas "Nanomedicine Molecular Science" (23107009) from the Ministry of Education, Culture, Sports, Science, and Technology, Japan (K. Gonda), and a Grant-in-Aid for Comprehensive Research and Development of an Early Stage Diagnosis Method and Instruments to Treat Cancer from New Energy and Industrial Technology Development Organization, Japan (K. Gonda, M. Watanabe, Y. Nakano, N. Ohuchi). We also acknowledge the support of the Biomedical Research Core of Tohoku University Graduate School of Medicine and Konica Minolta Science and Technology Foundation.

References

[1] A.M. Gown, Current issues in ER and HER2 testing by IHC in breast cancer, Modern Pathology 21 (2008) S8–S15.
[2] T. Moriya, N. Kanomata, Y. Kozuka, H. Hirakawa, I. Kimijima, M. Kimura, M. Watanabe, H. Sasano, T. Ishida, N. Ohuchi, J. Kurebayashi, H. Sonoo, Molecular morphological approach to the pathological study of development and advancement of human breast cancer, Medical Molecular Morphology 43 (2010) 67–73.
[3] S.V.D. Ven, V.T.H.B.M. Smit, T.J.A. Dekker, J.W.R. Nortier, J.R. Kroep, Discordances in ER, PR and HER2 receptors after neoadjuvant chemotherapy in breast cancer, Cancer Treatment Reviews 37 (2011) 422–430.
[4] A.S.-Y. Leong, Z. Zhuang, The changing role of pathology in breast cancer diagnosis and treatment, Pathobiology 78 (2011) 99–114.
[5] C. Thomas, J.-Å. Gustafsson, The different roles of ER subtypes in cancer biology and therapy, Nature Reviews Cancer 11 (2011) 597–608.
[6] D.S. Lidke, P. Nagy, R. Heintzmann, D.J. Arndt-Jovin, J.N. Post, H.E. Grecco, E.A. Jares-Erijman, T.M. Jovin, Quantum dot ligands provide new insights into erbB/HER receptor-mediated signal transduction, Nature Biotechnology 22 (2004) 198–203.
[7] A.V. Blaaderen, A. Vrij, Synthesis and characterization of colloidal dispersions of fluorescent, monodisperse silica spheres, Langmuir 8 (1992) 2921–2931.
[8] N.A.M. Verhaegh, A.v. Blaaderen, Dispersions of rhodamine-labeled silica spheres: synthesis, characterization, and fluorescence confocal scanning laser microscopy, Langmuir 10 (1994) 1427–1438.
[9] K. Gonda, T.M. Watanabe, N. Ohuchi, H. Higuchi, In vivo nano-imaging of membrane dynamics in metastatic tumor cells using quantum dots, Journal of Biological Chemistry 285 (2010) 2750–2757.
[10] Y. Hamada, K. Gonda, M. Takeda, A. Sato, M. Watanabe, T. Yambe, S. Satomi, N. Ohuchi, In vivo imaging of molecular distribution of the VEGF receptor during angiogenesis in a mouse model of ischemia, Blood 118 (2011) e93–e100.
[11] J. Stingl, C. Caldas, Molecular heterogeneity of breast carcinomas and the cancer stem cell hypothesis, Nature Reviews Cancer 7 (2007) 791–799.
[12] A. Marusyk, V. Almendro, K. Polyak, Intra-tumour heterogeneity: a looking glass for cancer?, Nature Reviews Cancer 12 (2012) 323–334